Journal of Microelectronics and Electronic Packaging (2009) **6**, 32-37

ISSN: 1551-4897

Hermetic Package for Optical MEMS

F. Seigneur,* Y. Fournier, T. Maeder, P. Ryser, and J. Jacot

Abstract—**This paper describes the design and fabrication of a hermetic LTCC package for an optical MEMS chip designed for space applications. The package ensured electrical and optical connections, mechanical positioning, atmosphere control, and finally low thermally induced stress on the MEMS during the final packaging operation. The package consisted of a 10-layer LTCC case with a recessed cavity for the MEMS chip, and a glass lid (with antireflection coating and thin-film metallization for soldering) for optical I/O. The chip was mechanically attached to the bottom of the cavity with a silicone adhesive, and electrically connected through gold wire bonds. The gold wire bonding pads were routed through the LTCC module to a MegArray BGA connector. Hermetic closure of the cavity was carried out by soldering the glass lid onto the case in a controlled atmosphere. The two main difficulties involved in such a package were the high electrical connection density (400 connections) and low-temperature hermetic sealing. LTCC design rules for small-pitch lines, thick- and thin-film materials selection, screen printing, lamination techniques, and soldering methods are described in this paper.**

Keywords—**Hermetic packaging, interconnections, LTCC, MOEMS, solder sealing**

Introduction

The field of microelectro-mechanical systems (MEMS) enjoys rapid growth. Such devices often need special and precisely controlled conditions to operate correctly (temperature, inert gas, I/O interfaces, etc.). Often, development is mainly focused on manufacturing the MEMS device, and the final packaging is thus neglected. When the device to be encapsulated is at an advanced design stage, it is difficult to propose a convenient packaging method that fulfils the required final specifications together with manufacturing constraints. Long-term hermeticity and low sealing temperature are often difficult to achieve. Add the need of high electrical conductor density and optical interface, and the problem is even harder to solve. This paper describes a case study where the proposed packaging solution fulfils several external functions, together with constraints due to the sensitivity to heat of the encapsulated MEMS.

The first part of this paper describes the device to be packaged and the functions to be fulfilled by the package. Then, design and manufacturing of the solution are described and discussed, focusing on critical operations. Finally, the methods used as well as potential improvements are discussed in the conclusion.

Manuscript received September 2008 and accepted April 2009
1EPFL, IMT, LPM, Lausanne, Switzerland
*Corresponding author; email: frank.seigneur@a3.epfl.ch

Description of the Problem

The device to be packaged was an optical MEMS device designed for space telecommunication applications [1]. It consisted of 128 micro mirrors; each mirror requires three electrical connections for its electrostatic actuation. The MEMS chip was 35 mm long and 13 mm wide. Several critical functions needed to be fulfilled by the package, including optical and electrical interfaces, atmosphere control and mechanical positioning. These functions are described below.

A. Electrical Connection

The MEMS chip had to be electrically connected to a control electronics, by 386 bonding pads placed on two of its long sides. The bonding pads had a width of 120 μm and a pitch of 150 μm. The space between two pads is 30 μm.

B. Optical Interface

The MEMS consisted of an array of micro mirrors and needed a glass lid to allow an optical link to the outside. The glass was coated on both sides with an antireflective coating.

C. Mechanical Positioning

The MEMS chip needed to be positioned precisely under an array of optical fibers.

D. Atmosphere Control

The micro mirrors had to operate in a dry atmosphere to ensure long-term device reliability and stability. Some damping was needed; they cannot reside in vacuum, but needed an environment with an inert gas at a controlled pressure.

E. Sensitivity to Temperature

The package had to ensure a low thermal budget on the MEMS during the sealing operation. The micro mirrors might have deformed when exposed to temperatures above 200°C.

F. Production Volume and Design Flexibility

The volume to be produced was low (10–20 packages), but it must be possible to increase this volume up to 100 packages per year. The design had to be flexible, as changes can occur in both design of the MEMS and of the package during the development.

Description of the Solution

Regarding the specifications described in the previous section, the following solution was proposed: the package was composed of two main parts. The base was made of LTCC (DuPont 951) [2], and a glass lid is soldered to the base (see Fig. 1 and Fig. 2).

The package was a 62 × 62 mm 10-layer LTCC base with a recessed cavity for the MEMS chip. The chip was glued in the cavity. The chip was connected through wire bonds, and the gold wire bonding pads were connected to a MegArray BGA connector [3] through electrical lines and vias. The electrical lines, vias, and bonding pads were screen printed on the green tape. The bottom of the package consisted of five tapes that received the screen printed tracks and bonding pads. These tapes were 114 µm thick. The walls of the cavity were formed by five tapes that were 254 µm thick.

The glass lid was soldered to the package, thus ensuring hermeticity. The glass received an antireflective coating. A metallic frame was evaporated onto the glass, in order to allow wettability of the solder on the glass. To reduce the thermal impact on the MEMS device during encapsulation, all high-temperature operations were done before gluing the MEMS chip in the cavity. The final operation (bonding and soldering of the glass lid) were made at low temperature, reducing the thermal impact on the MEMS device.

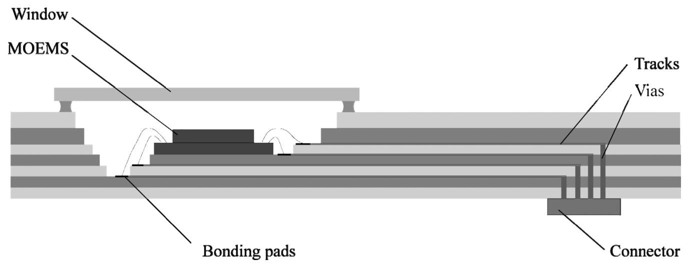

Fig. 1. Schematic view of the package.

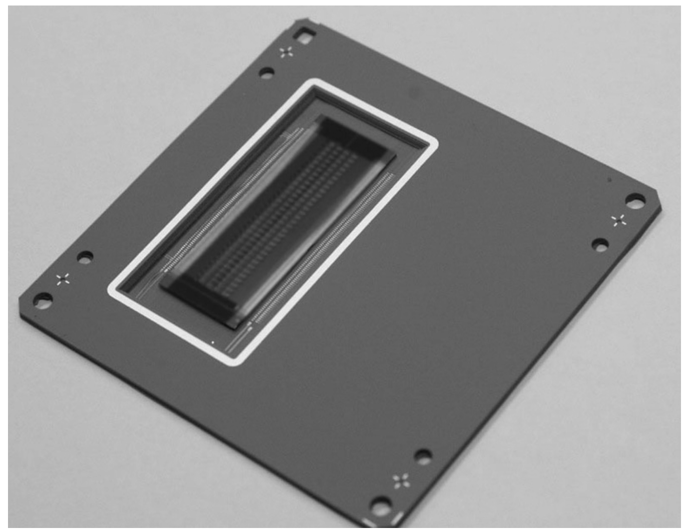
Fig. 2. Package with bonded chip, ready to be sealed.

Design

Although the design might seem simple, as it implied only conductor lines between the chip and the connector, the routing needed several design steps. They are described below.

A. Sketches

The first step was to determine the critical pitches. This led to a general routing. On the chip side, the bonding pads had a pitch of 150 µm. On the connector side, the pitch was 1,270 µm. There was a factor of 10 between the chip and the connector; the package had to make the link between these two domains. Standard screen printing allowed a minimum pitch of 300 µm (track width: 150 µm). This was convenient for the connector side, but a two-layer solution was needed on the chip side. In order to simplify routing, a four-layer solution was chosen that minimized the number of vias (see Fig. 1).

B. Use of Design Software

The second step was the design of the mechanical layout of the components, taking into account the previous remarks concerning the four layers needed (see Fig. 2). Routing was made in HYDE [4]. This software allowed for the design of modules on several layers, and also took shrinkage of LTCC into account. In our case, every track and via had to be drawn manually. The goal was to minimize the length of the tracks (see Fig. 3).

C. Design Rules

The fine pitch needed for screen printing was hard to obtain. Some design rules needed to be observed.

On the masks used for screen printing, the mesh was oriented at 45°. The tracks cannot be parallel to the mesh, because of resolution issues. The best screen printing resolution was obtained perpendicular to the screen printing direction, which means that the finest tracks must be parallel to the screen printing direction.

The via diameter was equal to the thickness of the tape (100 µm). To ensure a proper connection even with small misalignments, the via pad diameter was 200 µm. The MegArray connector cannot be soldered directly over the vias. The soldering pads must be slightly offset from the vias.

D. Paste Choice

Three different pastes fulfilling different functions were needed: bonding pads, tracks, and vias. The main concern was about bonding, as the equipment used allows only gold ball bonding. Therefore, the paste for the bonding pads also needed to be gold (CDF-34 or DP5472). For the tracks, two different pastes were tested: DP6146 (Ag-Pd) and DP6145 (Ag). Two via fill pastes were also tested: DP6138 (Ag-Pd) and DP6141 (Ag).

Concerning the via fill pastes, no significant difference was observed. The DP6141 was finally chosen. For the tracks, DP6146 exhibited better printability and compatibility during firing with the CDF-34 Au bonding pads, but implied more deformation during firing, especially for high track density zones, where the LTCC thickness was low.

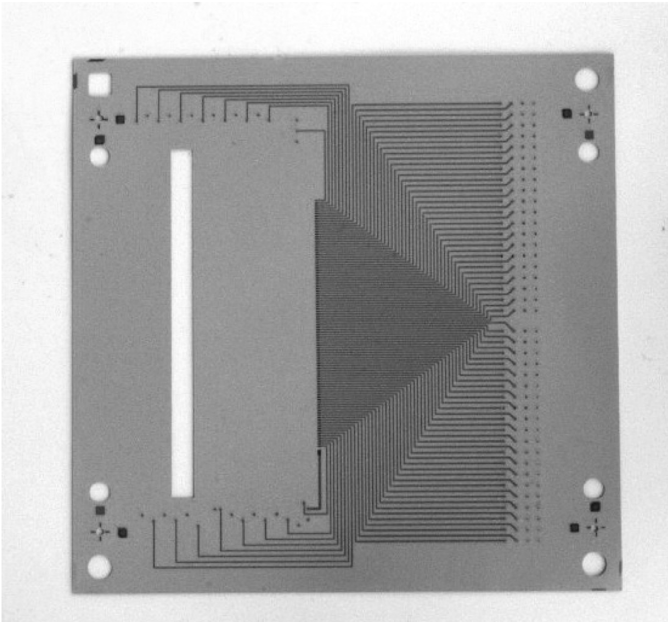

Fig. 3. Layout of tape 6.

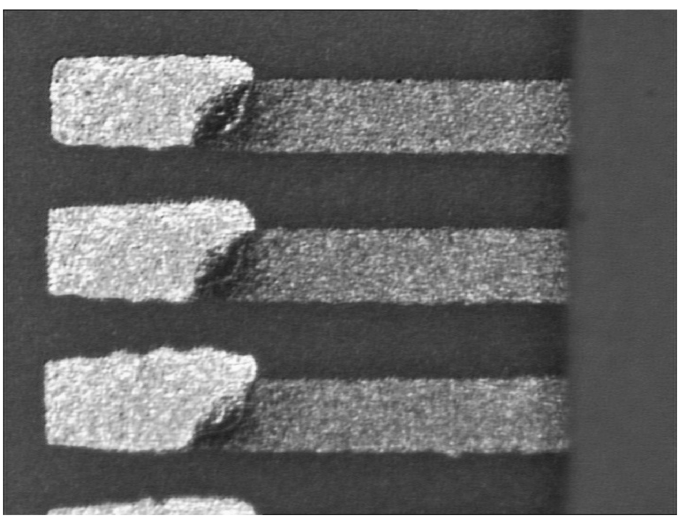

Fig. 4. Peeling between bonding pads (DP5472) and tracks (DP6146).

For the bonding pads, peeling was observed between the bonding pad and the track when using DP5472 (see Fig. 4). In the end, we chose CDF-34 for the bonding pads, DP6146 for the tracks, and DP6141 for the vias. The tested pastes are summarized in Table I. The final choice is marked in bold.

Table I
Summary of Pastes used for Screen Printing

Type	Paste	Material
Via fill (a)	**DP6141**	**Ag**
Via fill (b)	DP6138	Ag-Pd
Tracks (a)	DP6145	Ag
Tracks (b)	**DP6146**	**Ag-Pd**
Bonding pads (a)	**CDF-34**	**Au**
Bonding pads (b)	DP5472	Au

Manufacturing

The package follows the standard LTCC manufacturing steps: preconditioning, laser cutting, screen printing (vias, tracks, and pads), lamination, firing, and postfiring operations. Details are given on critical operations.

A. Screen Printing

Each tape required three screen printing operations (via fill, tracks, and bonding pads). The screen printed paste needed to be dried at 120°C for 5 min before each new screen printing operation. Due to the fine pitch, alignment was critical. The screen printer used was a semiautomatic Aurel C900 equipped with pattern recognition and manual alignment. Alignment marks were used, but functional alignment is preferred when possible.

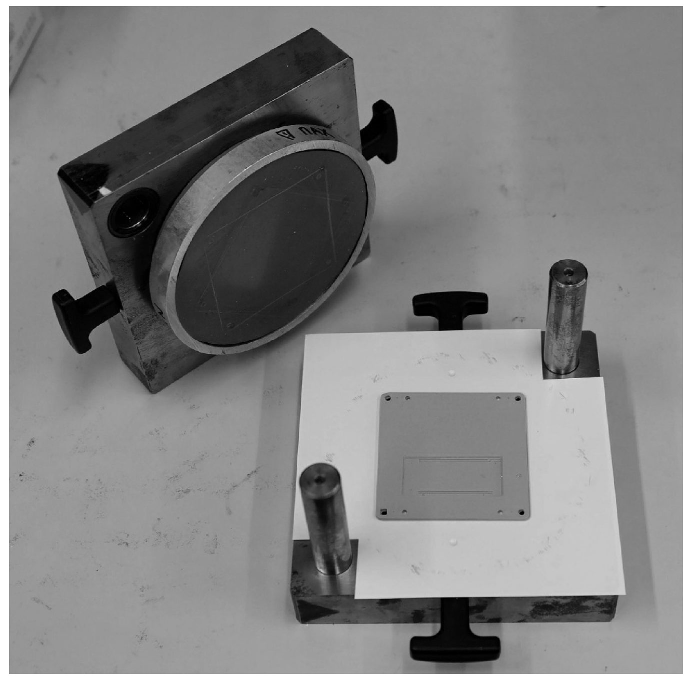

Fig. 5. View of LTCC stack before lamination. Note the constrained rubber plate.

B. Lamination

The cavity is deep (1 mm), and the bottom had to be well laminated. Several changes to standard lamination procedures were needed to achieve good lamination quality. The top plate was fitted with a thick rubber sheet to achieve pseudo-isostatic lamination of the bottom of the cavity (see Fig. 5). The tapes forming the cavity were cut so that the walls were tapered to form an angle of 45°. The first tests were made using an unconstrained 12 mm thick rubber plate, positioned between the lamination press and the LTCC stack. A mylar sheet protected the LTCC from the rubber and the press. The result was not reproducible; deformation of the laminated LTCC stack

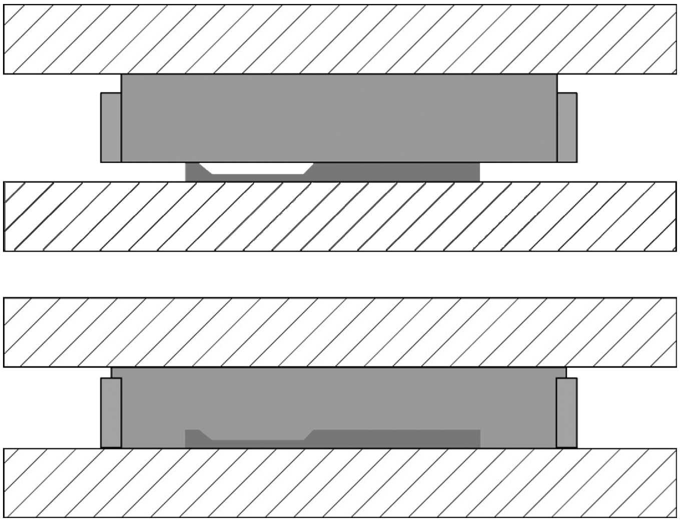

Fig. 6. Schematic view of the constrained rubber used for lamination.

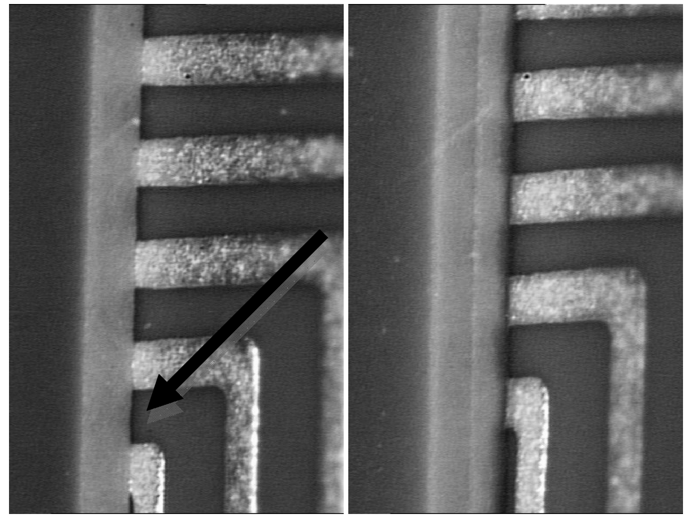

Fig. 7. Insufficient lamination (left); there is a gap between two LTCC layers; and good lamination (right).

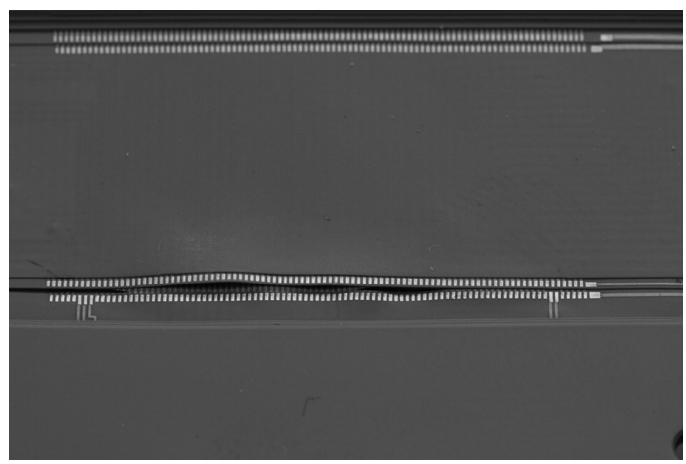

Fig. 8. Delamination of bonding pads.

occurred. When the rubber was compressed, its size in x and y increased, applying forces that deformed the LTCC stack. To prevent this, the rubber plate was constrained within a circular aluminum tube (see Fig. 6). The height of the rubber plate was slightly greater than the tube, allowing the rubber to be compressed by the lamination press. In this way, the deformation in x-y was minimal. To further improve the homogeneity of the pressure, a second rubber plate was cut to the size of the cavity and inserted before lamination.

The lamination pressure was 80 bars; most samples were laminated at ambient temperature (25°C) and some were laminated at 55°C, without a noticeable difference in the outcome. The mean shrinkage measured after firing was 14.1% and 13.7% in x and y, respectively. This must be compared with 12.7% expected in x and y, according to DuPont [2]. Previous work by Fournier et al. [5] showed an average shrinkage of 13.11%.

The use of the rubber during lamination allowed a good and reproducible lamination, using a much simpler process than isostatic lamination. However, there were some disadvantages: the top of the package was not perfectly flat as bumps corresponding to vias, tracks, and alignment marks could be seen on the top of the package.

Another issue concerning lamination is the high density of tracks. At some areas, the surface of the tracks was equal to the surface of the apparent LTCC. This led to deformation due to a different shrinkage coefficient between the paste and the LTCC. Further, ensuring good lamination in this case was not trivial, because the lamination pressure and temperature had to be limited to avoid excessive deformation of the package. To solve this, the surface of paste had to be reduced, and lamination had to be done with a rubber layer to ensure good lamination of the LTCC between the tracks (see Fig. 7).

Delamination was also observed during firing in a high track density zone (see Fig. 8). High track density implies a low overlap of LTCC. Such zones must be avoided or a way must be found to allow stronger lamination without deformation. It appears that the firing profile plays a role in delamination, especially the temperature ramp during sintering (see Fig. 9).

Delamination occurred on some samples for ramps of 1.5 K/min. The best results were observed for ramps of 2.5 K/min. The storage time between the last screen printing operation and lamination was also a factor that had an influence (up to two months storage time for samples showing delamination). This was due to the fact that the green tape dries out over time.

C. Post Operations

The window metallization (DP6135D) was screen printed and fired. Then an overglaze (ESL G481 or ESL G485-1, Pb-Free) was screen printed as a solder mask. Solder paste (Sn-Cu-Ag) was screen printed for bump formation. Finally, the MegArray connector was placed manually onto the package and reflowed in an oven.

D. Soldering of Glass Lid

A metallization layer is needed in order to obtain wettability of the Sn-Bi eutectic solder on the glass lid. Previous work

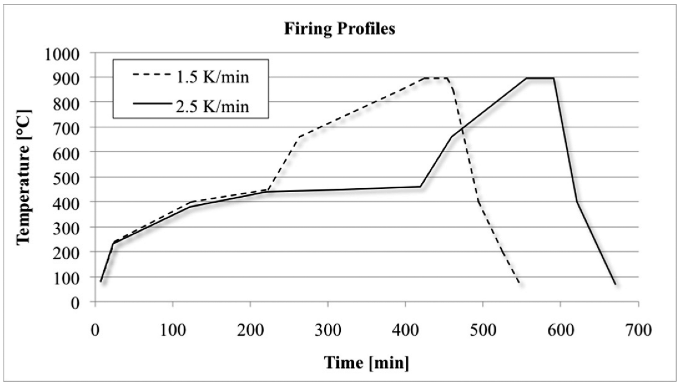

Fig. 9. Profiles used for firing.

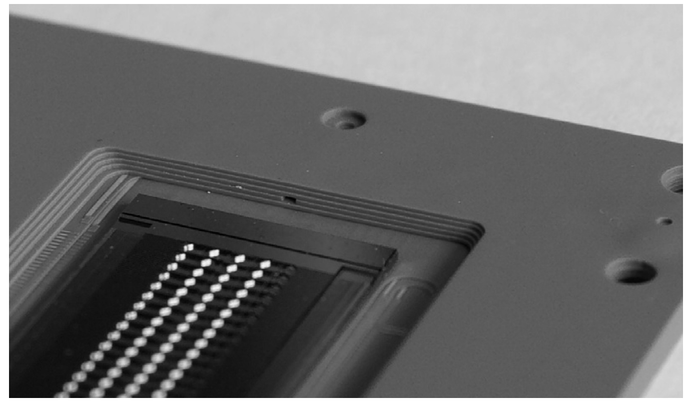

Fig. 10. Channel used to balance pressure during soldering.

showed that screen printed thick film worked well (ESL 590G-Ag), but the main drawback was the high required firing temperature (500°C): the antireflection coating was damaged at temperatures above 300°C. A low temperature solution was the evaporation of Ti (20 nm)-Pt (200 nm)-Au (50 nm) onto the glass. Thorough cleaning of the glass was found to be critical for achievement of good adhesion—sputtering might be less sensitive in this regard.

The Sn-Bi solder paste was manually dispensed on the metallic ring. It was first reflowed in an oven under vacuum in order to outgas the flux. The flux residue was then removed in an ultrasonic bath of TopKlean [6] for 15 min. Au ensures excellent solder wettability but must be kept thin in order to avoid the formation of brittle Au-Sn intermetallics [7].

Glue was dispensed in the cavity, and the chip was manually aligned on it. The glue (EPOTEK 353 ND, epoxy) was cured for 1 h at 80°C. Finally, the chip was wire bonded.

After gluing the chip in the cavity, all operations were done at low temperature (150°C or less), which ensured a minimal thermal impact on the chip. The soldering of the glass can be done in an oven, without risk of reflowing the MegArray connector, which was previously soldered with Sn-Cu-Ag (melting at ~220°C). The main drawback of Sn-Bi for soldering of the lid was sensitivity to creep at temperatures above 70°C [8–10]. Standard Sn-Pb solder could be used instead, as its reflow temperature (180°C) is still under that of Sn-Cu-Ag. A more elegant and efficient solution to the creep issue would be soldering of the lid with Sn-Cu-Ag also, using local laser heating.

When soldering the glass lid in an oven, the internal pressure due to the temperature of the gas inside the package might break the liquid solder joint, leading to a nonhermetic package.

To prevent this, a small channel was created in a wall of the package that balanced inside and outside pressures. The channel was cut in the tape (see Fig. 10). To avoid collapsing during lamination, a small piece of cardboard was inserted in the channel. This cardboard was easily burnt during firing. After soldering of the glass, when the whole package was cold, the channel was sealed by a small soldered cap that was heated locally.

Table II
Duration of Manufacturing Tasks

Task	Duration
Laser cutting	4 d
Screen printing on green tape	5 d
Lamination and firing	2 d
Screen printing	2 d
Gluing of chip and bonding	5 d
Electrical test and sealing	5 d

Table III
Cost of Material for a Batch of 10 Packages

Tape	Qty	Cost (with paste), €
1–5 (114 μm)	50	150
6–9 (254 μm)	40	120
10 (114 μm)	20	60
Totals	110	330 €

Potential Costs

An estimation of the development and manufacturing time is given in this section. The final cost for a batch of packages is composed of the design, the manufacturing, and the material. The case study is given for a batch of 10 packages.

A. Development and Design

Development time is related to complexity (i.e., number of connections) of the MEMS chip to be encapsulated, but also to its requirements (i.e., sensitivity to temperature, protective atmosphere needed). One must also determine the mechanical properties of the package: size, mounting holes, layout of components, and choice of the connector. In our case, one can estimate this time to four months, including drawing and layout in HYDE. This should be an iterative process with a close collaboration with the MEMS chip designer. Two persons are needed for this task, but their working rate is estimated at 50%.

B. Manufacturing

The manufacturing part consists of the manufacture of screens for screen printing, laser cutting, screen printing, stacking, lamination, firing, postfiring operations, gluing and bonding of the chip, electrical tests, and sealing. The times for these tasks is summarized in Table II.

C. Material

The material is a small part of the cost with regard to development and manufacturing. Nevertheless, the costs are summarized in Table III. This cost includes the LTCC base only; the connector and glass lid are not included. The cost for one tape is 3 € including the paste. The total material cost for one package is estimated to be approximately 33 €.

Conclusion and Future Work

The proposed solution fulfills all the functions needed. It can easily be adapted to similar MEMS devices. The low development and manufacturing costs, together with design flexibility, implies that this solution should be considered for MEMS packaging.

Routing all 386 connections to one connector is challenging. The use of several smaller connectors would simplify the routing process, as they could be more easily distributed on the surface of the package.

The routing of the package should be symmetrical. The form factor of the package implies deformation and delaminations. It would be wiser to increase the thickness of the package, and reduce its surface, placing the connector directly under the chip.

Hermeticity has yet to be measured. Previous measurements were done on similar packages (LTCC and soldered glass lid) [11]. A gas sensitive LTCC module developed by Maeder et al. [12] could easily be integrated in such a package.

Acknowledgments

The authors would like to thank Herbert Shea (EPFL, IMT, LMTS), Wilfried Noell (UniNE, IMT, Samlab) and Peter Herbst (Sercalo Microtechnology LTD, www.sercalo.com) for providing us the MOEMS chip.

References

[1] W. Noell, M. Zickar, and N. de Rooij, “Two-axis MEMS mirror for precise beam steering without feedback,” in Proceedings of the 6th ESA Round Table on Micro/Nano Technologies for Space, 2007.

[2] DuPont Green Tape 951 System, DuPont MCM, Microcircuit Materials, http://www2.dupont.com/MCM/en_US/.

[3] MegArray Connector 84740-102LF, FCI, http://www.fciconnect.com.

[4] HYDE, Durst CAD/Consulting GmbH, Holzgerlingen, Germany.

[5] Y. Fournier, L. Bieri, T. Maeder, and P. Ryser, “Influence of lamination parameters on LTCC shrinkage under unconstrained sintering,” in Proceedings of the 4th European Microelectronics and Packaging Symposium, IMAPS, pp. 165–170, 2006.

[6] TopKlean, Avantec Performance Chemicals, 94683 Vincennes CEDEX, France.

[7] J. Kalenik, R. Kisiel, A. Mlozniak, and Z. Szczepanski, “Some properties of SnAg and SnAgCu solder joints on printed circuit boards,” in Proceedings of the XXVIII International Conference of IMAPS, pp. 277–280, 2004.

[8] J. Villain, T. Qasim, J. Pahl, and H. Masuch, “Struktur und Eigenschaften von Vapor-Phase umgeschnolzenen SnBi- und SnZn-Lötverbindungen an SMD-Bauelementen,” IMAPS Deutschland Konferenz, München.

[9] F. Hua and J. Glazer, “Lead-free solders for electronic assembly,” in Proceedings of Design and Reliability of Solder Interconnects, TMS Symposium, pp. 65–73, 1997.

[10] Wei, Y., C. L. Chow, K.J. Lau, P. Vianco, H.E. Fang, “Behavior of lead-free solder under thermomechanical loading,” Journal of Electronic Packaging, Vol. 126, pp. 367–373.

[11] F. Seigneur, T. Maeder, and J. Jacot, “Laser soldered packaging hermeticity measurement using metallic conductor resistance,” in Proceedings of the XXX International Conference of IMAPS, 2006.

[12] T. Maeder, Y. Fournier, F. Seigneur, and P. Ryser, “LTCC active oxygen getter module for hermetic packaging applications,” in Proceedings of the IMAPS/ACerS 4th International Conference and Exhibition on Ceramic Interconnect and Ceramic Microsystems Technologies, 2008.